Research Article

Antimicrobial activity and FTIR spectral properties of some phosphate glasses and glass–ceramics from the system P_2O_5–NaF–CaF_2 and effects of dopants

Amany A. El-Kheshen[1] · Abeer A. Abd El Aty[2] · Nagwa A. Ghoneim[1] · Mohamed A. Marzouk[1]

Abstract
Ternary fluorophosphates glasses doped with one of oxides: CeO_2, ZnO, Ag_2O, La_2O_3 were prepared by the melt—annealing technique. Differential thermal analysis of the prepared samples was conducted to obtain the suitable temperatures for thermal heat treatment of the parent glasses to be able to convert them to their corresponding glass–ceramics. X-ray diffraction analysis was carried out to identify the formed crystalline phases within the glass–ceramics. FTIR spectral studies of the prepared glasses and glass–ceramic was done to find out the structural building groups in the studied samples; indicated that the vibrational bands due to phosphate groups are mainly Q^2 and Q^3. That is because of the high content of P_2O_5 (70%), besides the sharing of vibration due to (PO_3F) groups. FTIR of the glass–ceramics show sharp peaks correlated with the crystallinity with well-defined crystalline species and the changes of the intensities of the mid region absorption can be related to depolymerization effects. Antimicrobial activity of the doped glassy or glass–ceramic samples was assessed to justify their suitability as antimicrobial agents. Glassy samples revealed excellent antibacterial and antifungal effects as compared with glass–ceramics, and addition of Ag_2O showed the best broad spectrum antimicrobial activity even at low concentration (0.1%). CeO_2, La_2O_3 and ZnO exhibited good antibacterial activity and moderate antifungal effects when added to glassy samples.

Keywords Fluoro-phosphate · Glass · Glass–ceramics · FTIR · Antimicrobial activity

1 Introduction

Phosphate glasses belong to one of the most interesting vitreous systems which possess unique physical properties including high thermal expansion coefficients, low transition and softening temperatures and low preparation temperatures [1, 2]. The published data on the properties of basic metaphosphate glasses reveal extreme values depending mainly on the respective cations which have a large effect on the physical and chemical properties due to different bonding and structural arrangements [3]. The large differences between the values for cations with nearly the same radius (and coordination number), Zn^{2+} and Mg^{2+}, Fe^{3+} and Al^{3+}, show that there is no simple correlation with radius of the cation.

Some binary phosphate glasses exhibit anomalous behavior because of discontinuities in composition—property trends near the metaphosphate composition [4–6]. Phosphate glasses containing substantial fluorine content are known to be promising candidates for optical glasses with positive anomalous relative partial dispersion which reduces the chromatic aberration, color distortion and hence to obtain high resolution with microscopes and telescopes or other optical objectives [7].

Several authors [8–10] have studied borate glasses containing alkali or alkaline earth halide ions instead of the

✉ Amany A. El-Kheshen, aelkheshen1@yahoo.com | [1]Glass Research Department, National Research Centre, 33 EL Bohouth st. (former EL Tahrir st.). Dokki, Giza P.O.12622, Egypt. [2]Chemistry of Natural and Microbial Products Department, National Research Centre, 33 EL Bohouth st. (former EL Tahrir st.). Dokki, Giza P.O.12622, Egypt.

SN Applied Sciences (2019) 1:1016 | https://doi.org/10.1007/s42452-019-1048-5

Received: 29 May 2019 / Revised: 26 July 2019 / Accepted: 6 August 2019 / Published online: 10 August 2019

respective modifier oxides and have arrived to the conclusion that both types of glasses possess similar structural IR spectra. These authors have assumed that the fluoride containing glasses form tetrahedral fluoro–borate units (e.g. BO_3F) which have their IR vibrational modes within the same wavenumber range from 800 to 1200 cm^{-1} as familiar tetrahedral BO_4 groups.

Ehrt in her recent review article [3] has summarized its extensive studies with her colleagues on phosphate and fluoride phosphate glasses with the objective of selecting some distinctive and special glasses. The aim of their extended studies is the development of optical glasses suitable for lens design avoiding color distortion. These studies have indicated that fluorophosphate glasses are promising candidates. P–F bonding is required for anomalous dispersion. Some of these glasses doped with transition metal or rare earths have been investigated for the purpose of active laser, amplifier and photoluminescence glasses.

FT infrared absorption spectral studies of fluorophosphates glasses [11, 12] showed that the formation of nominated (PO_3F) groups could be recognized due to the sharing of alkali or alkaline earth fluorides with P_2O_5. Also, it has been suggested that the addition of modifiers of fluorides causes the formation of non-bridging fluorines of (NBF) as suggested by Shelby [13]. Such formed suggested groups and non-bridging fluorines are believed to bring some changes in the properties of the glasses due to the difference in field strength and bonding strength between fluorine and oxygen.

Glasses are considered to be materials of nonperiodic arrangements and do contain intrinsic defects (such as nonbridging oxygens, impurities, flaws) and can thus be affected by ionizing radiation (such as gamma rays, UV radiation) revealing induced radiation defects which can be identified by optical and ESR spectral studies. Glasses containing some transition metal ions (3d TM ions, WO_3, MoO_3) and also some rare some earth ions are identified to show some shielding behavior towards gamma irradiation [3, 12, 14–16]. Glass ceramics material is prepared via heat treatment of glass to arrange their atoms in order to form long-range order structure materials. Glass ceramic materials, having crystalline phases according to the structure of the parent glass, can be considered as a material with higher strength and higher durability than the amorphous glass.

The main objective of the present work is to find out the resistance effect of the prepared glass and their corresponding glass ceramics towards some kind of bacteria, yeast and fungi.

2 Experimental details

2.1 Preparation of the glasses

The studied glasses (Table 1) were prepared from the appropriate chemicals by melting in covered porcelain crucibles under ordinary atmosphere. Ammonium dihydrogen phosphate ($NH_4H_2PO_4$) was the source of P_2O_5, NaF and CaF_2 were introduced as such. Some selected oxides were introduced as additional dopants in the level (0.1% or 1%) including: the oxides CeO_2, La_2O_3, ZnO or Ag_2O as ($AgNO_3$).

Melting was carried out in SiC heated furnace (Vecstar, UK) at a temperature of 1000 °C for 90 min including rotation of the melts every 30 min to promote complete mixing and homogeneity. The finished melts were poured into slightly warmed stainless steel molds of required dimensions. The prepared glassy samples were immediately transferred to an annealing muffle regulated at 300 °C. The muffle was switched off after 1 h and left to cool with a rate of 30 °C/h to room temperature.

Table 1 Chemical composition (elements wt%) of the prepared glasses

Sample no.	Mol%			Added in wt%			
	P_2O_5	NaF	CaF_2	Ag_2O	CeO_2	La_2O_3	ZnO
Base	70	15	15	–	–	–	–
A1	70	15	15	0.1	–	–	–
A2	70	15	15	1	0	–	0
C1	70	15	15	–	0.1	0	–
C2	70	15	15	–	1		–
L1	70	15	15	–	–	0.1	–
L2	70	15	15	–	–	1	–
Z1	70	15	15	–	–	–	0.1
Z2	70	15	15	–	–	–	1

2.2 Differential thermal analysis behavior of the glasses

The differential thermal analysis behaviors of the finely powdered glassy samples were examined using SDTQ600 under N_2 gas. The powdered glasses were heated in alumina holder with another alumina holder as a reference material. The obtained results were used as a guide for determining the required heat-treatment temperatures, which were needed to induce complete and voluminous crystallization in the samples. Figure 1 illustrates the DTA thermograph of the undoped glass.

2.3 Preparation of the corresponding glass–ceramic derivatives

Glass samples were subjected to controlled thermal heat-treatment with a two-step regime. The glasses were first slowly heat-treated at a rate of 5 °C/min to reach 410 °C and kept at this temperature for 12 h which was sufficient to provide efficient nucleation sites. The muffle was then raised to reach 565 °C and kept at this second hold for 6 h to ensure complete crystallization of the samples. The muffle furnace with the samples inside was switched off and then left to cool to room temperature at a rate of 30 °C/h.

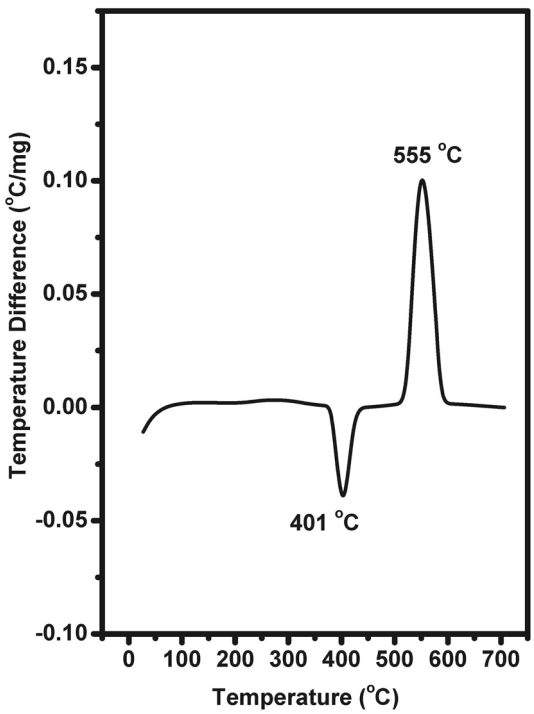

Fig. 1 Differential thermal analysis of the base glass

2.4 X-ray diffraction analysis

Identification of the formed crystalline phases during controlled heat-treatment was performed by X-ray diffraction analysis using a Bruker AXS diffractometer CD8-ADVANCE) with Cu-Ka radiation, operating at 40 kV and 10 mA. The diffraction data were recorded for 2θ values between 4° and 70° and the scanning rate was 10°/min.

2.5 Fourier transforms infrared absorption measurements (FTIR)

FT infrared absorption spectra of the prepared glasses and glass–ceramics were carried out at room temperature in the wave number range 400–4000 cm^{-1} by a Fourier transform computerized infrared spectrometer type (FTIR 4600 JASCO Corp. Japan) using the KBr disc technique. The samples were examined in the form of pulverized powder which was mixed with KBr with the ratio 1:100 mg sample powder to KBr, respectively. The weighed mixtures were then subjected to a pressure 5 tons/cm^2 to produce clear homogeneous discs. FTIR measurements were also carried out for the glass–ceramic derivatives as powder form.

2.6 Antimicrobial studies

2.6.1 Antibacterial activity test

Agar diffusion testing was used to evaluate the antibacterial activity of eight glass and glass ceramic samples according to the procedure given in [17]. The prepared samples containing Ag_2O, CeO_2, La_2O_3 or ZnO with two different concentrations (0.1 and 1 mol%) were investigated.

Antibacterial activity was evaluated against Gram positive (*Bacillus subtilis* ATCC6633) and Gram negative bacteria (*Escherichia coli* ATCC25922).the spore suspension of pathological strains was prepared and adjusted to be approximately (1×10^8 $spores^{-ml}$). 1 ml of spore suspensions was inoculated into each plate containing 50 ml of sterile nutrient agar medium (NA). After the media had cooled and solidified, 100 mg of the prepared powder samples were applied on the inoculated agar plates and incubated for 24 h at 30 °C. Diameters of zones of inhibition produced around the specimens were measured in (mm) at three different points and the average values are reported as Mean ± SD using MS Excel.

2.6.2 Antifungal activity test

Antifungal activity of the glass and glass ceramic samples were evaluated against pathogenic yeast (*Candida albicans* ATCC10321) and fungi (*Aspergillus niger* NRC53 and *Fusariumsolani* NRC15), by the agar diffusion technique

[18]. 1 ml of spore suspensions (1×10^6 spores^{-ml}) was inoculated into each plate containing 50 ml of sterile potato dextrose agar (PDA). 100 mg of the powder samples were applied on the inoculated agar plates after cooling and incubated for 72 h at 28 °C. The inhibition zone diameter (IZD) around samples was measured as mentioned above.

3 Results and discussions

3.1 Differential thermal analysis (DTA) and X-ray diffractions (XRD)

Figure 1 shows the differential thermal analysis of the prepared base undoped glass. The obtained data from the DTA pattern indicated a characteristic exothermic peak centered at about 555 °C which was applied to prepare the glass–ceramic derivatives.

Figure 2 exhibits the X-ray diffraction pattern of the base undoped glass ceramic as an example for the most probable formed phases after the treatment processes. The pattern reveals two characteristic identified phases of NaCa $(PO_3)_3$ and $Na_2Ca_4(PO_4)F$. The formed phases were accepted according to the chemical compositions of the prepared oxy-fluoride host phosphate glass.

3.2 FT infrared absorption spectra of glasses and glass–ceramic derivatives

Figures 3 and 4 illustrate the FTIR spectra of the studied glasses. The FTIR spectrum of the base undoped glass (Fig. 3) reveals the following spectral data after deconvolution due to the appearance of broad and composite bands

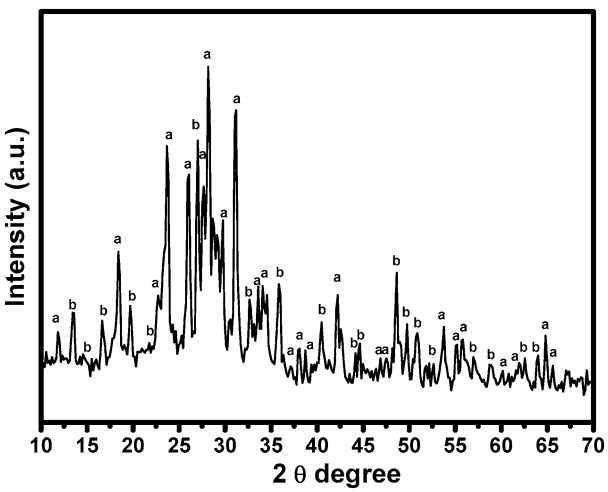

Fig. 2 X-ray diffraction pattern of the base glass ceramic where (a) NaCa $(PO_3)_3$ and (b) $Na_2Ca_4(PO_4)F$

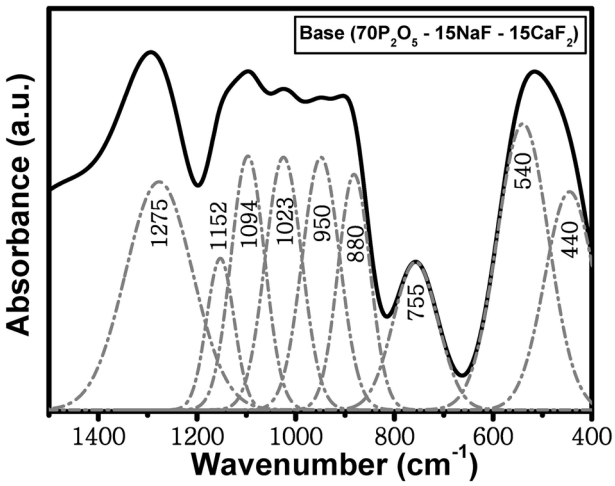

Fig. 3 FTIR absorption spectrum of the undoped base glass together with its deconvoluted spectrum

within the mid IR wavenumber range 400–1400 cm^{-1} after deconvolution:

a. A strong and broad far IR absorption band is observed showing splitting into two peaks at 440 and 540 cm^{-1}.
b. The appearance of a distinct medium band with a peak at 755 cm^{-1}.
c. A very broad and high distinguished composite band is identified extending from about 800 to 1200 cm^{-1} and enclosing five deconvoluted peaks at 880, 950, 1023, 1094 and 1152 cm^{-1}.
d. A last, an intense band is observed with a peak at 1275 cm^{-1}.

Figure 4 shows the FT infrared spectra of the doped glasses and the spectral details can be summarized as follows:

1. The glass containing 0.1% Ag_2O shows an IR spectrum similar to the spectrum of the undoped sample with overall lower intensity and the two far–IR bands exhibit more extension or broadness. The identified deconvoluted peaks are at 480, 581, 730, 785, 895, 985, 1080, 1130 and 1286 cm^{-1}. On increasing the Ag_2O to 1%, the IR spectrum of this identified glass is also very similar to that for the undoped glass.
2. The glass doped with 0.1% ZnO reveals an IR spectrum with distinct lower intensity to all the vibrational bands but the two far IR bands show broadness and the detailed identified deconvoluted peaks are at 410, 485, 558, 715, 773, 895, 988, 1079, 1131 and 1280 cm^{-1}. The doped glass containing 1% ZnO shows an IR spectrum similar to the spectrum of the undoped glass but

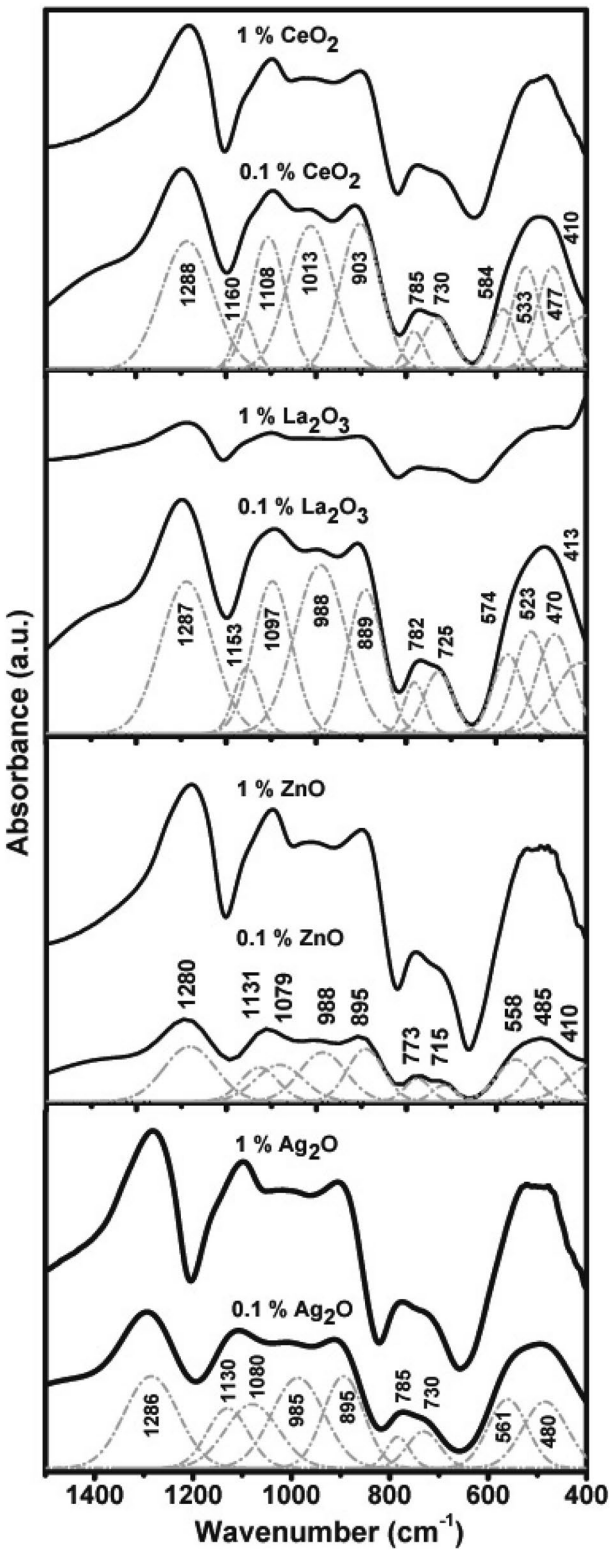

Fig. 4 FTIR absorption spectra of Ag, Zn, La and Ce—doped glasses

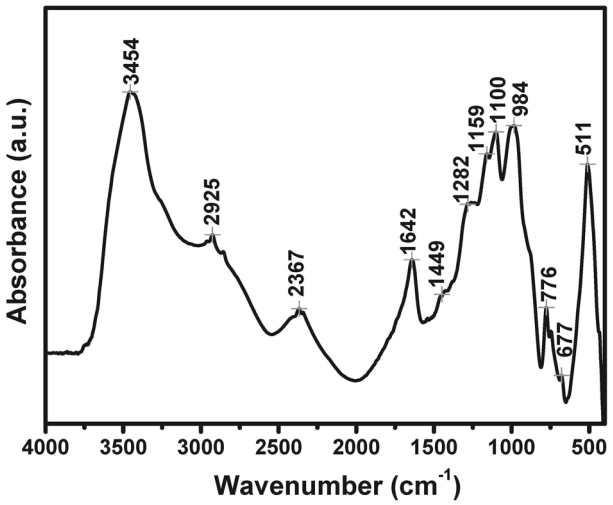

Fig. 5 FTIR absorption spectrum of the undoped base glass–ceramic

with the splitting of the two far IR bands to three peaks for the first and two peaks for the second band.

3. The glass doped with 0.1 La_2O_3 reveals IR spectrum closely similar to the undoped sample spectrum with only the extension of the two far IR bands. On increasing the La_2O_3 to 1%, the IR spectral curve highly decreases in intensity.
4. The IR spectrum of the glass containing 0.1% CeO_2 resembles that of the undoped sample and the same holds for the IR spectrum of the glass containing 1% CeO_2.

Figures 5 and 6 illustrate the FTIR spectra of the undoped base and doped glass ceramics. The IR spectrum of the base glass ceramic (Fig. 5) reveals pronounced sharp spectral peaks extending from 400 to 4000 cm^{-1}. The details of the IR spectrum of the base glass are summarized as follows:

(a) A very sharp and high distinct far–IR band is identified at 511 cm^{-1}.
(b) Three small bands are observed with peaks at 677, 705, 776 cm^{-1}.
(c) A very broad intense band is identified extending from about 800 to 1500 cm^{-1} and revealing five peaks at 984, 1100, 1159, 1282 and 1449 cm^{-1}.
(d) A sharp medium band is observed with peak at 1642 cm^{-1}.
(e) The small peaks are observed at 2367, 2880 and 2925 cm^{-1}.
(f) A broad and intense IR band extending from about 3000 to 3750 cm^{-1} is identified with a peak at 3454 cm^{-1}.

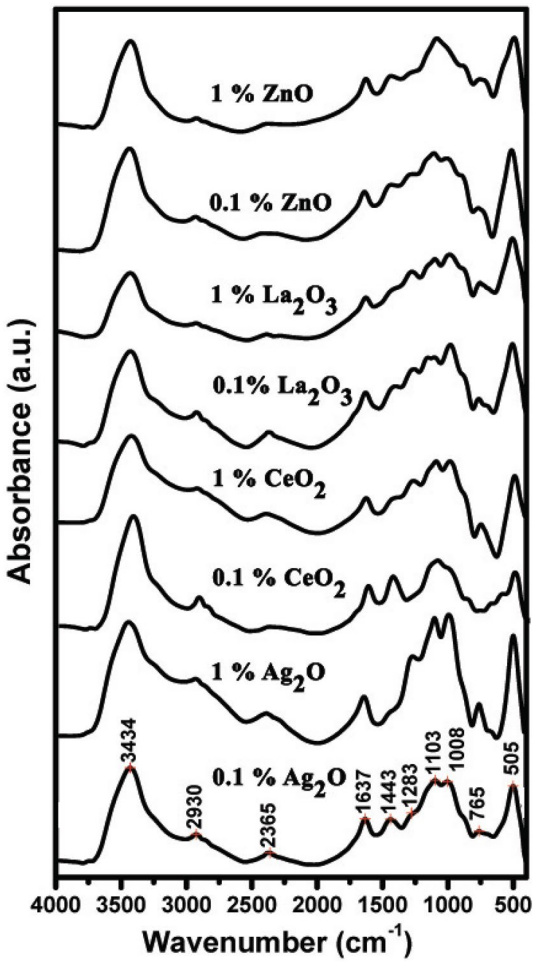

Fig. 6 FTIR absorption spectra of Ag, Ce, La and Zn—doped glass–ceramics

Figure 6 illustrates the IR spectra of the doped glass–ceramic samples. The spectral curves are almost repetitive and resembling that of the base but with some minor variations summarized as follows:

1. The bands at 505, 1637, 2365, 2930 and 3434 cm^{-1} are persistent in all samples without any changes.
2. The mid broad band extending from about 800 to 1500 cm^{-1} reveals some changes in the intensities of some component peak.

Experimental deconvoluted IR spectrum of the undoped base glass illustrates vibrational bands which are virtually related to phosphate groups and can be realized and interpreted on the following parameters [6, 19–22]:

(a) The chemical composition of the base glass consists of main glass forming oxide of P_2O_5 70% and the rest are modifiers of alkali or alkaline earth fluorides (15% NaF–15% CaF_2) and it is therefore expected that the vibrational modes are based on phosphate groups.
(b) The far IR band at 440 cm^{-1} is related to bending vibrations of O–P–O units, $\delta(PO_2)$ modes of metaphosphate chain groups.
(c) The strong band at 540 cm^{-1} is considered to be due to harmonics of bending vibrations of O=P–O linkages.
(d) The medium band at 755 cm^{-1} may be due to P–O–P symmetric stretching vibrations of metaphosphate groups.
(e) The bands at 880 and 950 cm^{-1} are correlated with asymmetric stretching modes of P–O–P linkages.
(f) The bands at 1023 and 1094 cm^{-1} are related to asymmetric stretching of P–O–P groups, ν_{as} (P–O–P) modes linked to metaphosphate.
(g) The bands at 1152 cm^{-1} are related to asymmetric stretching of PO_2 groups.
(h) The band at 1275 cm^{-1} is related to stretching vibrations of the doubly bonded oxygen (ν_{as} (P=O)).
(i) It is suggested that the presence of fluoride ions (NaF, CaF_2) causes or initiates the formation of some $(PO_3F)^{2-}$ as suggested by different authors [23, 24] within the glass network and vibrating within the wavenumber range 700–1300 cm^{-1}.

3.3 Antimicrobial properties of prepared glasses and glass ceramics

3.3.1 Antibacterial activity

The antibacterial activity of glass and their corresponding glass ceramics samples were studied against pathogenic bacteria *B. subtilis* (ATCC6633) and *E. coli* (ATCC25922). The results shown in Table 2 and Fig. 7 revealed that, the inhibition effect of samples containing Ag_2O against Gram positive and Gram negative bacteria were higher than other samples and base sample. The two concentrations of Ag_2O showed good effect against bacterial strains with IZD in range from 24 to 26 mm. The wide range of antibacterial activity of silver against Gram positive and Gram negative bacteria was mentioned previously by Abd El Aty and Ammar [25]. There are many mechanisms attributed to the bactericidal activity of silver, where they can influence both physical and chemical phenomena of microbial cells inhibiting the growth of microorganisms.

Also, samples which contain low and high concentrations of ZnO displayed good antibacterial activity against Gram negative bacteria with IZD in range from 23 to 25 mm, better than the Gram positive *B. subtilis* and base samples. Similar effects of zinc oxide on *E. coli* were observed by Zhang [26] and Adams [27] who reported the great ability of zinc oxide to damage the bacterial cell wall,

Table 2 Antimicrobial activity of the prepared glasses towards some (bacteria and fungi)

Glass	Inhibition zone diameter (IZD) (mm)				
	Gram positive bacteria	Gram negative bacteria	Yeast	Fungi	
	B. subtilis ATCC6633	*E. coli* ATCC 25,922	*C.albicans* ATCC 10,321	*A.niger* NRC53	*F.solani* NRC18
Base	16 ± 0.4	20 ± 0.8	13 ± 0.02	NA	25 ± 1.4
A1	24 ± 0.8	25 ± 1.1	15 ± 0.9	18 ± 0.06	30 ± 2.3
A2	26 ± 0.6	26 ± 1.5	25 ± 1.3	32 ± 1.1	33 ± 1.9
C1	15 ± 0.07	17 ± 0.4	13 ± 0.5	14 ± 0.9	20 ± 1.2
C2	16 ± 0.09	19 ± 0.5	15 ± 0.1	14 ± 0.07	25 ± 0.8
L1	14 ± 0.3	14 ± 0.9	14 ± 0.01	15 ± 0.09	20 ± 0.9
L2	18 ± 0.11	19 ± 1.2	15 ± 0.07	16 ± 1.3	26 ± 2.1
Z1	18 ± 0.7	23 ± 2.8	13 ± 0.8	NA	15 ± 1.5
Z2	20 ± 0.9	25 ± 0.7	16 ± 0.06	NA	15 ± 1.0

NA No activity

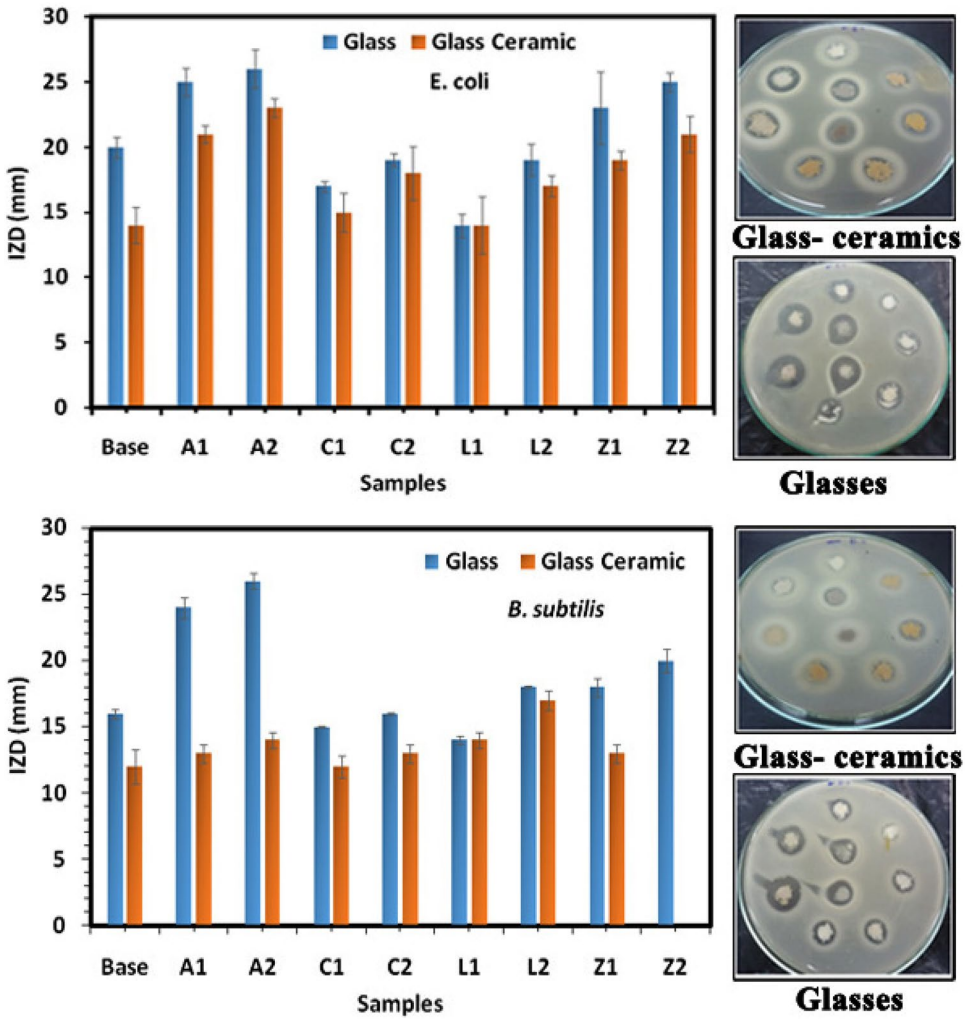

Fig. 7 Antibacterial activity of the prepared glasses and their corresponding glass–ceramics

followed by their accumulation in *E. coli* preventing their ability for multiplication. Results also revealed that other samples containing CeO_2 or La_2O_3 with different concentrations have moderate antibacterial activities. The degree of susceptibility of all tested bacteria to the eight samples can be arranged as the following order samples containing $Ag_2O > ZnO > CeO_2 \geq La_2O_3$, in comparison with the base.

On the other hand, the antibacterial assay of glass ceramic samples (Table 3 and Fig. 8) showed moderate activity with all bacterial strains when compared with glass samples. Glass ceramic containing Ag inhibits the growth of *B.subtilis*and *E. coli* better than the others with inhibition zones 13 and 23 mm, respectively. Glass ceramic containing CeO_2 and ZnO inhibited the activity of the gram negative *E.coli* better than the gram positive bacteria. But the samples containing La_2O_3 has the same effect (IZD, 14 and 17 mm) on two bacterial strains.

The obtained results confirm the description of Iždinský [28] that showed the high toxic effect of silver oxide compared to the zinc-oxide. It can be seen from a stronger suppression of both bacteria even at the application of lower Ag concentration.

3.3.2 Antifungal activity

Prepared glass samples with two different concentrations were tested for their antifungal activity against *C. albicans* (ATCC10321), *A. niger* (NRC53) and *F. solani* (NRC15). Results in Table 2 and Fig. 9 revealed that all samples showed good wide range of antifungal activities against the three tested fungi except samples containing ZnO showed high inhibition attitude against *C. albicans* and *F. solani* only with IZD of 16 and 15 mm, respectively. Sample containing high concentration of Ag_2O showed excellent antifungal activity against the three tested strains with IZD in range from 25 to 33 mm better than base sample. Results also indicated that samples containing low concentrations of CeO_2 and

Table 3 Antimicrobial activity of the prepared glass–ceramics

Glass–ceramic	Inhibition zone diameter (IZD) (mm)				
	Gram positive bacteria	Gram negative bacteria	Yeast	Fungi	
	B. subtilis ATCC6633	*E. coli* ATCC 25,922	*C.albicans* ATCC 10,321	*A.niger* NRC53	*F.solani* NRC18
Base	12 ± 1.3	14 ± 1.4	NA	NA	14 ± 0.7
A1	13 ± 0.7	21 ± 0.7	14 ± 1.1	14 ± 0.8	22 ± 0.6
A2	14 ± 0.6	23 ± 0.7	18 ± 0.7	26 ± 0.7	23 ± 1.4
C1	12 ± 0.8	15 ± 1.5	NA	NA	15 ± 1.5
C2	13 ± 0.7	18 ± 2.1	NA	NA	17 ± 0.7
L1	14 ± 0.6	14 ± 2.2	NA	NA	NA
L2	17 ± 0.7	17 ± 0.8	NA	NA	NA
Z1	13 ± 0.7	19 ± 0.7	NA	NA	16 ± 0.7
Z2	NA	21 ± 1.4	NA	NA	16 ± 0.7

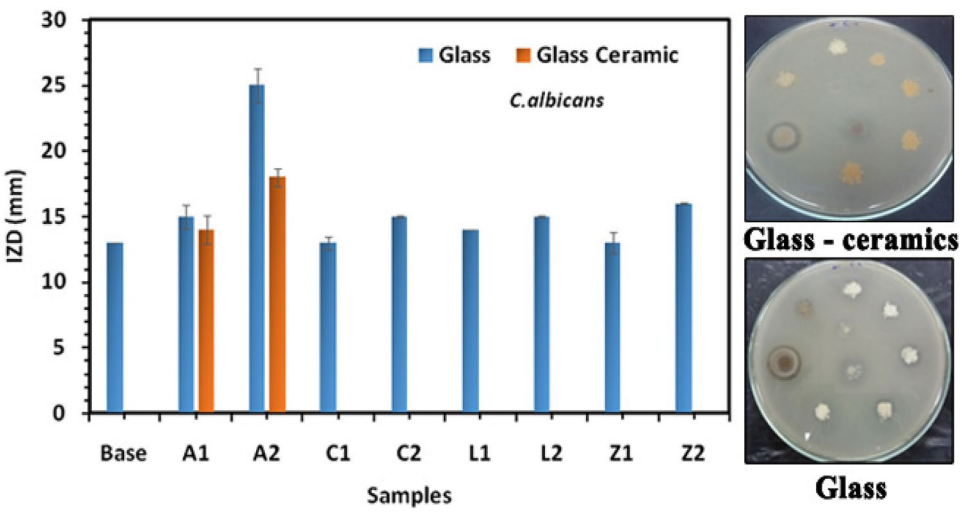

Fig. 8 Anti-yeast activity of the prepared glasses and their corresponding glass–ceramics

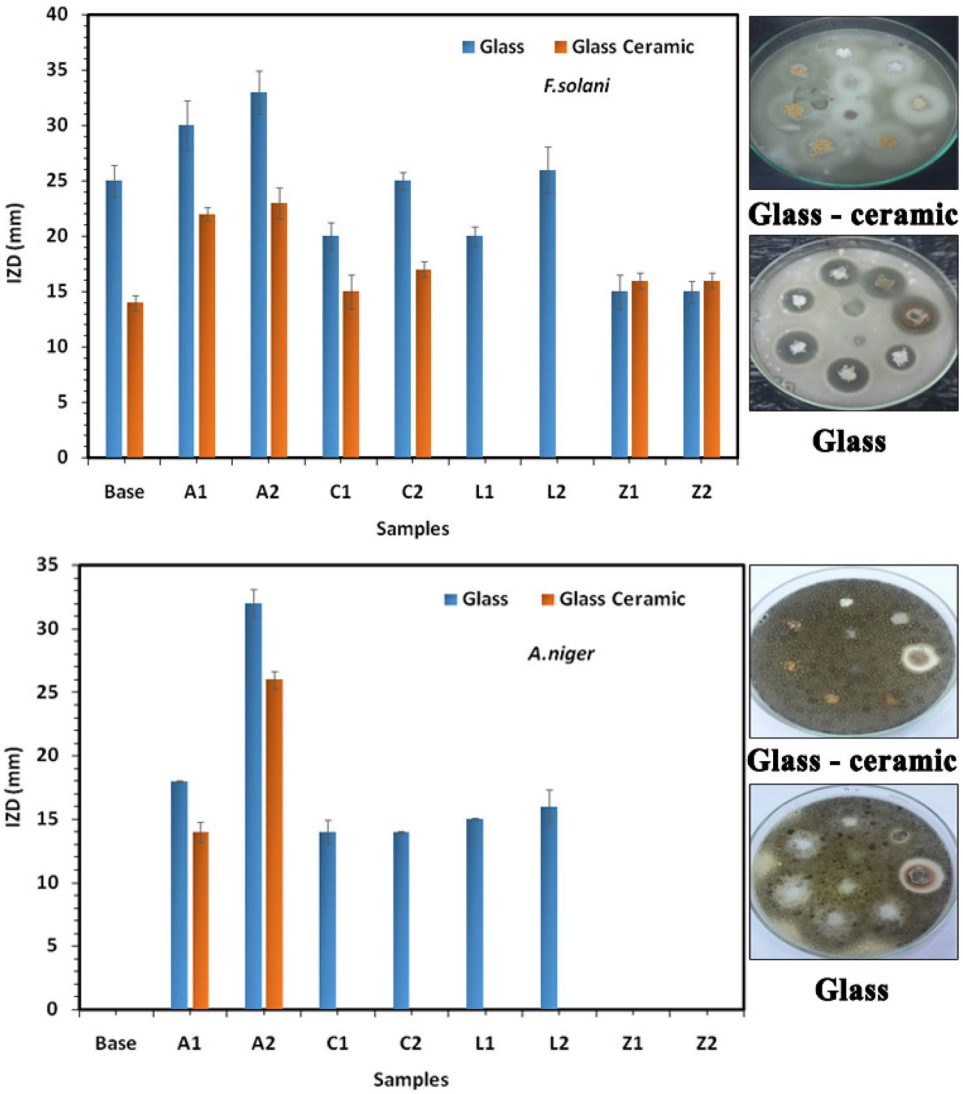

Fig. 9 Antifungal activity of the prepared glasses and their corresponding glass–ceramics

La_2O_3 have weak effects against fungi with IZD in range from 13 to 20 mm, that is nearly similar to the base samples. Increasing the concentrations of CeO_2 and La_2O_3 improved their inhibitory activities in range from 16 to 26 mm, that's better than base samples especially with the fungus *A. niger* which resistant to base sample and affected only by addition of CeO_2, La_2O_3 and Ag_2O to the composition. The fungicidal activity of theses metals is mainly caused by disrupting membrane potential of yeast cell and effects on the fungal mycelia [29].

Antifungal assay of eight glass ceramic and the base Table 3 showed no activity against *C.albicans* and *A.niger*, except the samples containing Ag inhibited the growth of the three fungi with IZD in range from 14 to 26 mm. Glass ceramic containing CeO_2 and ZnO showed week inhibitory effect against *F. solani* in range from 15 to 17 mm but, there's no antifungal effect for glass ceramic containing La_2O_3.

In conclusion, the results obtained from Table 2 and 3 indicated that the glasses showed the best antimicrobial activity against all tested bacteria and fungi.

4 Conclusion

Flourophosphate glass and glass ceramics were successfully prepared via melting—annealing method and heat treatment regime respectively. The parent glass was doped with CeO_2, ZnO, Ag_2O, La_2O_3 to study their anti microbial effects on different organisms. The functional groups were approved via FTIR instrument, the crystalline phases was detected via XRD pattern which were NaCa $(PO_3)_3$ and $Na_2Ca_4(PO_4)F$. The glass and glass–ceramic samples were investigated for their antibacterial and antifungal efficiency and the results were observed to be varied depending on the type of introduced oxides. Ag_2O offered a wide

range of antimicrobial activity at two different concentrations (0.1 and 1%). ZnO exhibited inhibition zone diameter in range from 18 to 25 mm against bacteria when introduced into glassy samples and from 13 to 21 mm when introduced into glass–ceramics. Samples contained CeO_2 and La_2O inhibited the Gram positive and Gram negative bacteria better than pathogenic *C. albicans* and *A. niger*.

Compliance with ethical standards

Conflict of interest On behalf of all authors, the corresponding author states that there is no conflict of interest.

References

1. Martin SW (1991) Ionic conduction in phosphate glass. J Am Ceram Soc 47(8):1767–1784
2. Brow RK (2000) Review: the structure of simple phosphate glasses. J Non Cryst Solids 263/264:1–28
3. Ehrt D (2015) Phosphate and fluoride phosphate optical glasses—properties, structure and applications. Phys Chem Glasses Eur J Glass Sci Technol B 56(6):217–234
4. Kordes E, Vogel W, Feterowsky R (1953) Physical chemistry investigations of the characteristics and fine structures of phosphate glasses. Z Eleckrochem 57(4):282–289
5. Kubo T, Cha J, Takebe H, Kuwabara M (2009) Thermal properties and structure of zinc phosphate glasses. Phys Chem Glasses Eur J Glass Sci Technol B 50(1):15–18
6. Smith CE, Brow RK (2014) The properties and structure of zinc magnesium phosphate glasses. J Non Cryst Solids 390:51–58
7. Ehrt D (1992) Structure and properties of fluoride phodphate glass. SPIE 1761:213–222
8. Shelby JE, Baker LD (1998) Alkali fluoroborate glasses. Phys Chem Glasses 39(1):23–28
9. Doweidar H, El-Damrawi G, Abdelghany M (2013) Structure and properties of CaF2–B2O3 glasses. J Mater Sci 47(9):4028–4035
10. ElBatal FH, Marzouk MA, Hamdy YM, ElBatal HA (2014) Optical and FT infrared absorption spectra of 3d transition metal ions doped in NaF-CaF_2-B_2O_3 glass and effects of gamma irradiation. J Solid State Phys 2014:1–9
11. Bocharova TV, Vlasova AN, Karapetyan GO, Maslenninkova ON, Sirotkin SA, Tagil'tseva NO (2010) Influence of small additives of rare-earth elements on the structure of fluorophosphate glasses. Glass Phys Chem 36:286
12. Marzouk MA, Hamdy YM, ElBatal HA, EzzElDin FM (2015) Photoluminescence and spectroscopic dependence of fluorophosphate glasses on samarium ions concentration and the induced defects by gamma irradiation. J Luminescence 166:295–303
13. Shelby JE (2005) Introduction to glass science and technology, 2nd edn. The Royal Society of Chemistry, Cambridge
14. ElBatal FH (2007) Gamma ray interaction with bismuth silicate glasses. Nucl Instr Methods Phys Res B 265:321–335
15. Elbatal FH, Marzouk SY, EzzElDin FM (2010) Gamma-ray interactions with WO3-doped sodium phosphate glasses. J Non Cryst Solids 356:2750–2759
16. ElBatal FH, Ibrahim S, Abdelghany AM (2012) Optical and FTIR spectra of NdF3-doped borophosphate glasses and effect of gamma irradiation. J Mol Struct 1030:107–112
17. Abd El-All AS, Osman SA, Roaiah HMF, Abdalla MM, Abd El Aty AA, AbdEl-Hady WH (2015) Potent anticancer and antimicrobial activities of pyrazole, oxazole and pyridine derivatives containing 1,2,4-triazine moiety. Med Chem Res 24:4093–4104
18. El-serwy WS, Mohamed NA, El-serwy WS, Kassem EMM, Abd El Aty AA (2015) Synthesis of new benzofuran derivatives and evaluation of their antimicrobial activities. Res J Pharm Biol Chem Sci 6:213–224
19. Abdel Kader AA, Higazy A, Elkholy MM (1991) Compositional dependence of infrared absorption spectra studies for TeO2-P2O5 and TeO2-P2O5-Bi2O3 glasses. J Mater Sci Mater Electron 2:57
20. Efimov AM (1997) Vibrational spectra, related properties, and structure of inorganic glasses. J Non Cryst Solids 109:209
21. Moustafa YM, El-Egili K (1998) Infrared spectra of sodium phosphate glasses. J Non Cryst Solids 240:144–153
22. Rao PS, Rajyasree C, Babu AR, Teja NV, Rao PK (2011) Effect of Bi2O3 proportion on physical, structural and electrical properties of zinc bismuth phosphate glasses. J Non Cryst Solids 357:3585–3591
23. Möncke D, Ehrt D, Velli LL, Varsamis CPE, Kamitsos EI (2005) Proceedings of the VII European society glass science and technology conference, Athens, Greece, April 2004, Physics and Chemistry of Glasses, 46(2):67–71.
24. Marzouk MA, Hamdy YM, ElBata HA, EzzElDin FM (2015) Photoluminescence and spectroscopic dependence of fluorophosphate glasses on samarium ions concentration and the induced defects by gamma irradiation. J Luminescence 166:295–303
25. Abd El Aty AA, Ammar HA (2016) Potential characterization and antimicrobial applications of newly bio-synthesized silver and copper nanoparticles using the novel marine-derived fungus *Alternaria tenuissima* KM651985. Res J Biotechnol 11(8):71–82
26. Zhang L, Jiang Y, Ding Y, Povey M, York D (2007) Investigation into the antibacteria behaviour of suspensions of ZnO nanoparticles (Zn nanofluids). J Nanopart Res 9:479–489
27. Adams LK, Lyon DY, Alvarez PJJ (2006) Comparative eco-toxicity of nanoscale TiO2, SiO2, and ZnO water suspensions. Water Res 40:3527–3532
28. Iždinský J, Reinprecht L, Nosáľ E (2018) Antibacterial efficiency of silver and zinc oxide nanoparticles in acrylate coating for surface treatment of wooden composites. Wood Res 63(3):365–372
29. Kim KJ, Sung WS, Suh BK, Moon SK, Choi JS, Kim JG (2009) Antifungal activity and mode of action of silver nanoparticles on Candida albicans. Biometals 22:235–242